Multi-probe conductance formulae for mesoscopic superconductors

1993 J. Phys.: Condens. Matter 5 4187

(http://iopscience.iop.org/0953-8984/5/25/009)

J. Phys.: Condens. Matter 5 (1993) 4187–4206. Printed in the UK

Multi-probe conductance formulae for mesoscopic superconductors

C J Lambert†, V C Hui‡ and S J Robinson†

† School of Physics and Materials, Lancaster University, Lancaster LA1 4YB, UK
‡ Defence Research Agency, Electronics Division, Malvern WR1 3PS, UK

Received 1 February 1993

Abstract. After presenting an intuitive picture of quasi-particle transport in mesoscopic superconductors, which emphasizes the intimate relation between Andreev scattering and zero resistivity, we develop a general theory of DC transport in mesoscopic normal–superconducting structures. Generalized multi-probe conductance formulae are derived, which take into account not only the effect of Andreev scattering on transport coefficients, but also the non-conservation of quasi-particle charge which arises in the presence of a superconducting condensate. Experiments on quasi-particle charge imbalance are described naturally by this approach.

1. Introduction

At a low enough temperature, or for small enough systems, a quasi-particle such as an electron or hole can pass through a sample without scattering inelastically. In this mesoscopic limit, the phase coherence of quasi-particles is preserved and transport properties depend in detail on the diffraction pattern produced by elastic scattering from inhomogeneities and boundaries. During the past decade, the study of normal mesoscopic systems has led to the discovery of a range of new phenomena, including universal conductance fluctuations [1,2], quantized conductance of point contacts [3,4] and the detection of macroscopic changes in transport coefficients arising from tunnelling within a single atomic two-level system [5].

Until recently, these advances had centred almost exclusively on normal mesoscopic systems. However during the past few years, the hitherto distinct fields of mesoscopic physics and superconductivity have come together, leading to the possibility of a range of new developments involving hybrid normal–superconducting structures. One class of such systems is typified by mesoscopic Josephson junctions, which arise when a mesoscopic weak link is formed between two non-mesoscopic superconducting contacts. For such structures, the critical current I_c is predicted to exhibit a range of new quantum phenomena. Recent examples are the discretization of the critical current through a ballistic point contact [6], the appearance of a universal resonant Josephson current through quantum dots [7] and the prediction of universal supercurrent fluctuations in diffusive point contacts [8].

Another class of hybrid systems arises when the superconductor itself is mesoscopic. This arises when a small superconducting sample is connected to the outside world through normal external leads, or when superconducting islands are immersed in a normal mesoscopic background. In such systems, transport properties such as electrical or thermal conductances exhibit new effects which are absent from their normal counterparts. For

0953-8984/93/254187+20$07.50

example, the electrical conductance of a sample containing two superconducting islands is predicted to vary periodically with the phase difference of the islands, even when the Josephson coupling between the islands is negligibly small [9–11]. Another example is the prediction of superconductivity-induced Anderson localization [12–14] in long strips, where quasi-particles above the bulk energy gap can become localized by spatial fluctuations in a superconducting order parameter.

This paper is aimed at deriving multi-probe conductance formulae, which form a starting point for examining a range of new effects associated with this second class of structures. Many of these effects arise because of the fundamental difference between quasi-particle transport and electrical conductance in the presence of a superconducting condensate. In section 2, this is emphasized by presenting an intuitive picture of charge transport, which provides new insight into the question of why the presence of an energy gap in a BCS superconductor implies zero resistivity. In section 2, we note that such a gap leads to Andreev scattering and argue that if the latter occurs in steady state, then zero resistivity is an immediate consequence.

The argument presented in section 2 is important, because it suggests that modern approaches to transport in normal mesoscopic systems should form a useful starting point for understanding transport in the presence of superconductivity. However, since current theories of transport in normal mesoscopic structures do not differentiate between quasi-particle diffusion and charge transport, it is clear that the fundamental conductance formulae at the heart of these theories must be modified. In [15] current–voltage relations needed to modify both the Landauer formula [16, 17] and the two-probe Büttiker formula [18] were written down. In sections 3 and 4, a generalization of this treatment is presented, which not only yields appropriately modified multi-probe conductance formulae, but also provides a natural framework for describing measurements of quasi-particle charge imbalance [19–21] in mesoscopic structures.

The multi-probe formulae derived in sections 3 and 4, which form the central results of this paper, express multi-probe conductances in terms of S-matrix coefficients. In [9], 'golden rules' for Andreev scattering were derived, which express S-matrix elements in terms of scattering solutions to the Bogoliubov–de Gennes equation. Generalizations to multi-probe systems are presented in appendix A.

2. Andreev scattering and superconductivity

In this section, an intuitive picture is presented, which underpins the more formal analysis appearing in later sections. This picture illustrates the intimate relationship between Andreev scattering and superconductivity and demonstrates why the energy gap of a superconductor can lead to a vanishing resistivity. To this end, consider first an ideal one-dimensional free-electron gas in a box of size L. At zero temperature, the free-electron energy levels $E_k = \hbar^2 k^2/2m$ are filled up to the chemical potential μ, as shown in figure 1(a). Figure 1(b) shows excited states of such a system with the same number of electrons, produced by removing an electron from a state q with energy $E_q < \mu$ and placing it in a state p, with $E_k > \mu$. The change in momentum of the system is $\Delta k = p - q$, while the change in energy is $\Delta E = E_p - E_q = (E_p - \mu) + (\mu - E_q)$. Since each of the quantities in the parentheses is positive, it is conventional to define quasi-particle excitation energies $\epsilon_k^0 = |E_k - \mu|$ so that $\Delta E = \epsilon_p^0 + \epsilon_{-q}^0$. The subscript $-q$ in the second term is again conventional and recognizes the fact that the change in momentum of the system can be regarded as a change $+p$ associated with the electron added to p and a change $-q$ associated with the electron removed from q, the latter being equivalent to a hole added to state $-q$. These quasi-particle dispersion relations, which express the change in energy of the system as a function of the change in system momentum, are shown in figure 1(*c*), along with the locations of the above particle-like and hole-like excitations. Since k now represents the system momentum, it is clear that the group velocity $v_k^0 = \hbar^{-1}\partial_k\epsilon_k^0$ of a particle-like (hole-like) excitation is parallel (anti-parallel) to its wavevector.

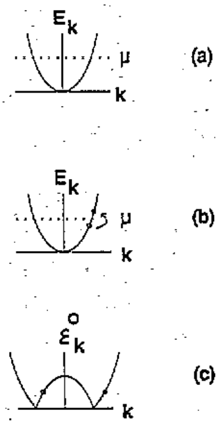

Figure 1. (*a*) The parabolic energy spectrum for a non-interacting system of electrons in one dimension. (*b*) An excitation formed by removing an electron below the Fermi level μ and placing it into a higher energy state. (*c*) The corresponding quasi-particle excitation spectrum.

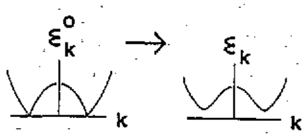

Figure 2. A BCS energy gap arises when cusps in the free-electron quasi-particle dispersion curve become rounded.

In terms of the excitation picture of figure 1(*c*), a superconducting transition is merely an expression of the fact that nature dislikes a singularity and therefore at a low enough temperature a phase transition occurs, which rounds the cusps at $E = 0$. For the simplest case of an s-wave weak-coupling superconductor, this yields the dispersion relation shown in figure 2, where

$$\epsilon_k = [(\epsilon_k^0)^2 + |\Delta|^2]^{1/2}. \tag{2.1}$$

Clearly, such a dispersion relation can only be written down when k is a good quantum number. More generally, there exists a spatially varying superconducting order parameter $\Delta(x)$ which vanishes in the normal phase. In most physical situations the coherence length ξ, which sets the scale for spatial variations in $\Delta(x)$, is much larger than the typical inverse wavevector k_F^{-1} of a quasi-particle, where k_F is defined by $\mu = \hbar^2 k_F^2/2m$. Consequently qualitative results can be obtained using quasi-classical arguments, with $|\Delta(x)|$ acting as a local energy gap.

To answer the question of why the existence of a non-zero $\Delta(x)$ implies zero resistivity, it is necessary to understand how excitations are (Andreev) reflected at an interface between a normal metal and a superconductor. First, recall how the reflection of an electron at a normal potential barrier $U(x)$ is described quasi-classically. As shown in figure 3(*a*), an incident electron of energy E is reflected at a classical turning point, where the local wavevector $k(x) = \hbar^{-1}\sqrt{[2m(E - U(x)]}$ vanishes. In this picture the electron slides down a sequence of local parabolic dispersion curves, until at the turning point it passes through the dispersion minimum and both the group velocity and momentum are reversed. Andreev reflection [22] at a normal–superconducting (N–S) interface can be understood through a similar argument. By definition, $\Delta(x)$ vanishes in the normal material and achieves its bulk value $\Delta(\infty)$ deep inside the superconductor. In the absence of other potential variations at the interface, the reflection of a quasi-particle can again be described by a sequence of local dispersion relations, as shown in figure 3(*b*). Again, the classical turning point arises when a quasi-particle of fixed energy, slides around the minimum of a local dispersion curve and reverses its group velocity. In contrast with normal reflection, the momentum is almost unchanged, whereas the character of the excitation has changed from being particle-like to hole-like. In two dimensions, the reflection process is shown in figure 3(*c*). In k space an incident particle outside the Fermi circle evolves into a hole inside the Fermi circle. In real space, all components of the group velocity are reversed and the N–S boundary acts like a phase conjugate mirror.

These essential differences between normal and Andreev scattering immediately imply that there is a fundamental difference between charge transport in superconducting and normal materials. To highlight an important consequence of this, first consider charge transport though a normal mesoscopic material. A typical viewpoint adopted when describing such a system in one dimension is shown in figure 4(*a*), which depicts a scattering region of length L connected by perfect external leads to the outside world. If a unit particle flux is incident from the left, then at equilibrium the only possible outgoing fluxes are a transmitted flux on the right and a reflected flux on the left. The intensities of these fluxes are T_0 and R_0 respectively and satisfy $R_0 + T_0 = 1$. The current in the left lead is clearly $I = e(1 - R_0)$, where e is the electronic charge. If the scattering region contains a finite fraction of impurities, then it is well known that as $L \to \infty$, $T_0 \to 0$. Consequently $R_0 \to 1$, $I \to 0$ and therefore the electrical resistance diverges. In contrast, if $\Delta(x)$ is non-zero within the scattering region, two new possibilities of Andreev transmission and Andreev reflection arise, as shown in figure 4(*b*). If the intensities for these processes are T_a and R_a respectively, then $R_0 + T_0 + R_a + T_a = 1$ and since a reflected hole moving to the left produces a current to the right, the current in the left lead is $I = e(1 - R_0 + R_a)$. The relative strengths of different scattering processes depend on the microscopic structure of an interface and only for the ideal boundary considered in figure 3(*b*) will normal reflection processes be small. As $L \to \infty$ one again finds that all transmission coefficients vanish, so that $R_0 + R_a = 1$. However, at equilibrium, provided $R_a \neq 0$, the current does not vanish and therefore the electrical resistance no longer diverges. In practice, since the reflection of a quasi-particle wavepacket takes place in a boundary layer of finite extent, R_a and R_0 will approach constant values as $L \to \infty$ and therefore the resistance *per unit length* will vanish.

The above argument is not quite complete, because to obtain an equilibrium situation in which the charge on the superconductor does not change with time, one must consider the effect of a second current carrying lead, connected to the right of the scatterer. This will be taken into account in the following section and does not change the above result. To summarize, the presence of a non-zero energy gap leads to the possibility of Andreev scattering and the occurrence of the latter in steady state implies that a current can flow through a dirty material, whose resistance would otherwise diverge. Of course, an energy gap is not necessary for the onset of superconductivity. Andreev scattering can arise even in the absence of an energy gap, provided there exists an order parameter which couples particles to holes. For this reason, it is the latter rather than the former that is crucial to superconductivity.

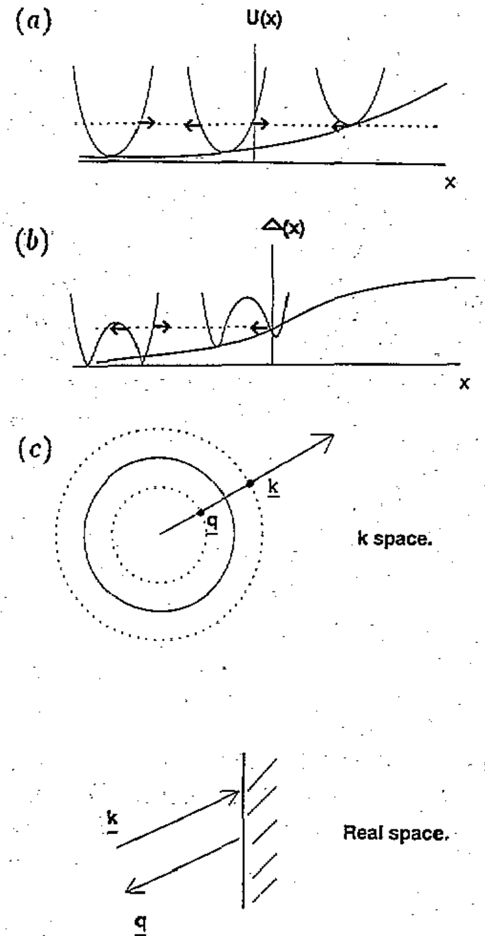

Figure 3. (*a*) Quasi-classical reflection of an electron by a potential barrier. (*b*) The corresponding picture leading to Andreev reflection at a normal–superconducting interface. In more than one dimension, (*c*) shows Andreev reflection in *k* space and real space.

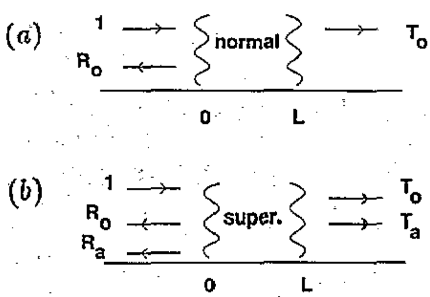

Figure 4. (*a*) Transmission and reflection of normal electrons in one dimension. (*b*) The additional Andreev processes, which arise in the presence of superconductivity.

The above argument demonstrates that, while diffusive properties of quasi-particles may not be qualitatively different from those of normal systems, the physics of charge transport is grossly affected. This implies that many of the standard formulae used to describe charge transport in normal mesoscopic media must be modified. To illustrate this, we now quantify the above arguments by deriving generalizations of standard formulae for multi-probe conductances of mesoscopic systems in the presence of Andreev scattering.

3. Multi-probe conductance formulae in the presence of Andreev scattering

Consider an arbitrary scatterer S containing a superconducting region of chemical potential μ, connected to n external reservoirs by ideal normal current-carrying leads, as shown in figure 5. If the chemical potentials of the reservoirs are $\{\mu_i\}$ and the currents $\{I_i\}$, then in the linear response regime the currents are related to the small quantities $\{\mu_i - \mu\}$ by an expression of the form

$$I_i = \sum_{j=1}^{n} a_{ij}(V_i - V) \tag{3.1}$$

where if e is the electronic charge, $V_j - V = (\mu_j - \mu)/e$. For a normal non-interacting system, one can show that $\sum_{i=1}^{n} a_{ij} = \sum_{j=1}^{n} a_{ij} = 0$. In this case the potential V does not affect the right-hand side of (3.1) and when all $\{\mu_i\}$ are equal, all currents vanish. These conservation laws are implicit in the derivation of conductance formulae for normal systems and reflect the fact that, in the absence of inelastic scattering, only external potential differences induce charge flow . In contrast, for an interacting system, and in particular when Andreev scattering is present, they no longer hold, because the scattering region can act as a source or sink of quasi-particle charge. As a consequence all conductance formulae are modified and we are led to identify the quantities

$$x_i = \sum_{j=1}^{n} a_{ij} \tag{3.2}$$

and

$$y_j = \sum_{i=1}^{n} a_{ij} \tag{3.3}$$

as the natural variables which quantify this change. In section 4, the relation between a_{ij} and scattering matrix elements will be considered, but for the purpose of obtaining generalized conductance formulae the values of these coefficients need not be specified.

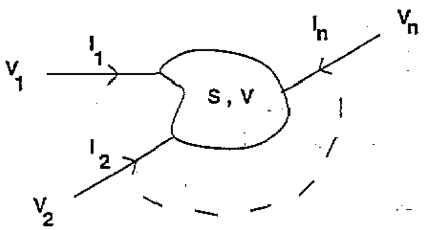

Figure 5. A scatterer S with condensate potential V, connected to n normal current-carrying leads.

For the equipotential case of $V_i = V'$ for all i, (3.1) yields $I_i = x_i(V' - V)$ and therefore a non-current carrying state is achieved only when the condensate potential V equals the external potential V'. This is an example of a general feature of the theory of [15] and its expanded version below; namely for a given set of external potentials, the condensate potential must be determined self-consistently to achieve a steady state solution. The problem of determining the steady state distribution of the internal degrees of freedom of a scatterer must be faced by any theory of transport in the presence of interactions. However, for a system in which quasi-particle interactions arise through Andreev scattering only, this problem is simplified, because only a small number of parameters is needed to specify the state of a superconducting condensate and only one of these (V) explicitly enters linear response formulae for transport coefficients. The existence of a unique steady state condensate potential is a key feature, without which (3.1) could not be written down.

If the cofactor matrix of a_{ij} is b_{ij}, then inverting (3.1) yields $(V_i - V) = d^{-1}\sum_{j=1}^{n} b_{ji} I_j$, where d is the determinant of the matrix a_{ij}. For the experimental case of interest, where only two probes α and β carry current, we write $I_\alpha = -I_\beta = I$ and $I_i = 0$ for $i \neq \alpha, \beta$, to yield

$$V_i - V = I(b_{\alpha i} - b_{\beta i})/d. \tag{3.4}$$

From this expression, the conductance $G_{ij}^{\alpha\beta} = I/(V_i - V_j)$ is given by

$$G_{ij}^{\alpha\beta} = d/d_{ij}^{\alpha\beta} \tag{3.5}$$

where

$$d_{ij}^{\alpha\beta} = b_{\alpha i} - b_{\beta i} + b_{\beta j} - b_{\alpha j} \tag{3.6}$$

From (3.4), the voltages are given by

$$V_i - V = G_{kl}^{\alpha\beta}(V_k - V_l)(b_{\alpha i} - b_{\beta i})/d = (V_k - V_l)(b_{\alpha i} - b_{\beta i})/d_{kl}^{\alpha\beta}. \tag{3.7}$$

Equations (3.5)–(3.7) are very general results, which we shall illustrate by considering the two- and three-probe formulae in detail. For a normal system where $d = 0$, we shall see that the denominator on the right-hand side of (3.5) also vanishes and consequently, in the limit $x_i \to 0$, $y_i \to 0$, the ratio is well defined. In contrast the potentials $V_i - V$ will be shown to depend sensitively on the manner in which the limit is approached.

The two-probe formula is implicit in the analysis of Lambert [15] and has been written down explicitly in [9]. For $n = 2$, (3.5) yields

$$\begin{aligned} G_{12}^{12} &= (a_{11}a_{22} - a_{21}a_{12})/(b_{11} - b_{21} + b_{22} - b_{12}) \\ &= (a_{11}a_{22} - a_{21}a_{12})/(a_{22} + a_{12} + a_{11} + a_{21}). \end{aligned} \tag{3.8}$$

Since the denominator of this expression is $x_1 + x_2$ and the numerator is $a_{11}(x_1 + x_2) - x_1 y_1 = a_{22}(x_1 + x_2) - x_2 y_2$, one finds

$$G_{12}^{12} = a_{11} - x_1 y_1/(x_1 + x_2) = a_{22} - x_2 y_2/(x_1 + x_2). \tag{3.9}$$

Note that, since the determinant of the matrix a_{ij} is guaranteed to vanish when x_i, $y_i \to 0$, the expression for G_{12}^{12} possesses a vanishing denominator in this limit. Nevertheless, as illustrated by (3.9), the conductance is well behaved, because the denominator is multiplied by a term which is second order in x_i, y_i. Consequently in the 'non-interacting normal limit', where $x_i, y_i \to 0$, the second term on the right-hand side of (3.9) vanishes, to yield the two-probe Büttiker conductance

$$G_{12}^{12} \to a_{11} = a_{22}. \tag{3.10}$$

An interesting consequence of the minus sign in (3.9) is that the switching on of superconductivity, parametrized by increasing $\{x_i, y_i\}$ from zero, can cause G_{12}^{12} to either increase *or decrease*.

The quantity $\mu = eV$, which in the presence of superconductivity is identified with the condensate chemical potential, is obtained by noting that (3.7) yields $V_1 - V = (V_1 - V_2)(b_{11} - b_{21})/d_{12}^{12}$ and $V_2 - V = (V_1 - V_2)(b_{12} - b_{22})/d_{12}^{12}$, which combine to yield

$$V = V_1 + (V_1 - V_2)y_1/(y_1 + y_2). \tag{3.11}$$

Since the numerator and denominator in the second term on the right-hand side are both linear in y_i, the limit that these quantities vanish can only be obtained by computing them explicitly and then taking the limit. This suggests that, for a system near its transition temperature, the voltage V may be much more sensitive to fluctuations than the conductance G^{12}_{12}.

In the literature [23–29], a great deal of attention has focused on the boundary resistance between a normal 'lead' and a superconductor. In general, since reflection and transmission coefficients are non-local, the resistance of a superconductor connected to a normal leads cannot be uniquely divided into two separate boundary resistances. One exception to this arises in the limit of zero transmission, where $a_{12} = a_{21} = 0$ and (3.9) reduces to

$$G^{12}_{12} = [1/a_{11} + 1/a_{22}]^{-1}. \tag{3.12}$$

Hence the two-probe resistance $[G^{12}_{12}]^{-1}$ reduces to a sum of two boundary resistances $R_1 = a_{11}^{-1}$, $R_2 = a_{22}^{-1}$ associated with the left and right leads respectively. In section 4, it will be shown that these are precisely the boundary resistances derived by Blonder and co-workers [24].

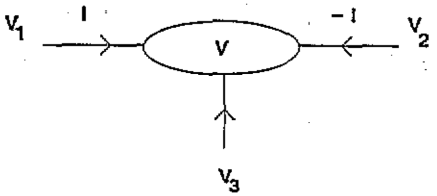

Figure 6. A three-probe system, in which lead 3 carries no current.

Having analysed the two-probe conductance in detail, we now turn to the case of three external reservoirs. An interesting class of experiments, measuring quasi-particle charge imbalance, are closely related to the three-probe system of figure 6. In the case of no transmission between probes 1 and 3 and probes 2 and 3, where $a_{13} = a_{31} = a_{23} = a_{32} = 0$, equation (3.4) yields $V_3 - V = 0$. Hence if probe 3 makes contact deep inside the superconductor, in a region where no quasi-particles from reservoirs 1 and 2 are transmitted, then V_3 measures the condensate chemical potential $\mu = eV$. More generally, if quasi-particles can be transmitted into probe 3, $V_3 - V$ is non-zero and can be interpreted as the potential difference between quasi-particles and the condensate arising from quasi-particle charge imbalance [19–21]. For such a system one obtains from (3.5)

$$G^{12}_{12} = \frac{[a_{11}a_{33} - a_{13}a_{31}][x_1 + x_2 + x_3] - x_3y_3a_{11} - x_1y_1a_{33} + x_1y_3a_{31} + x_3y_1a_{13}}{a_{33}[x_1 + x_2 + x_3] - x_3y_3}. \tag{3.13}$$

This is a somewhat cumbersome result, which can be rewritten in many equivalent forms. The choice (3.13) makes explicit those terms which are quadratic in the small quantities x_i, y_i and can therefore be neglected in the normal limit. In this limit, (3.13) yields

$$G^{12}_{12} \to [a_{11}a_{33} - a_{13}a_{31}]/a_{33} \tag{3.14}$$

and in the limit of no transmission into probe 3, the two-probe formula (3.10) is recovered.

For this three-probe configuration, (3.7) yields for the potential difference due to charge imbalance

$$V_3 - V = (V_1 - V_2)(b_{13} - b_{23})/d_{12}^{12} = (V_1 - V_2)[a_{32}y_1 - a_{31}y_2]/[a_{33}(x_1 + x_2 + x_3) - x_3 y_3]. \tag{3.15}$$

As noted above, if $a_{32} = a_{31} = 0$, then $V_3 = V$ and probe 3 measures the condensate potential. In common with (3.11), both the numerator and denominator are linear in the quantities x_i, y_i and therefore the normal limit can only be taken after explicit evaluation of these parameters.

4. Calculation of transport matrix elements a_{ij}

To obtain expressions for transport matrix elements a_{ij} of (3.1), we first relate them to S-matrix elements, by analogy with standard approaches to DC transport in normal disordered systems. For a system with a given normal potential $U(\boldsymbol{r})$, vector potential $\boldsymbol{A}(\boldsymbol{r})$ and order parameter $\Delta(\boldsymbol{r})$, the reflection and transmission coefficients of a quasi-particle of energy E are obtained by solving the Bogoliubov–de Gennes equation

$$\boldsymbol{H}(\boldsymbol{r})\Psi(\boldsymbol{r}) = E\Psi(\boldsymbol{r}) \tag{4.1}$$

where

$$\boldsymbol{H}(\boldsymbol{r}) = \begin{pmatrix} -\frac{\hbar^2}{2m}\left(\nabla - \frac{ie\boldsymbol{A}(\boldsymbol{r})}{\hbar c}\right)^2 - \mu + U(\boldsymbol{r}) & \Delta(\boldsymbol{r}) \\ \Delta^*(\boldsymbol{r}) & \frac{\hbar^2}{2m}\left(\nabla + \frac{ie\boldsymbol{A}(\boldsymbol{r})}{\hbar c}\right)^2 + \mu - U(\boldsymbol{r}) \end{pmatrix}. \tag{4.2}$$

In the region occupied by ideal external leads, we choose $\Delta(\boldsymbol{r}) = U(\boldsymbol{r}) = \boldsymbol{A}(\boldsymbol{r}) = 0$.

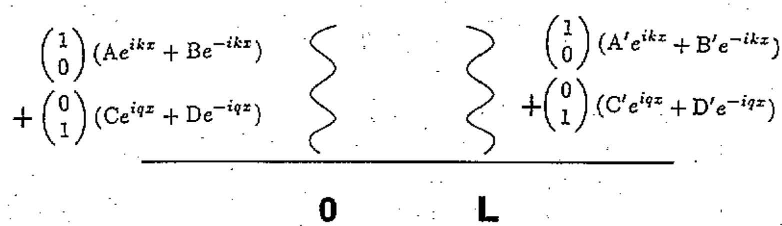

Figure 7. In one dimension, the most general solution to the Bogoliubov–de Gennes equation consists of incoming and outgoing plane waves in the external leads.

At large distances from the scattering region, for d-dimensional leads of constant cross section, the general solution of this equation reduces to the sum of a finite number of plane waves, associated with the quantization of transverse modes within the external 'waveguides'. For plane waves of energy E, the ith lead will possess $m_i(E)$ incoming and $m_i(E)$ outgoing channels associated with distinct transverse wavevectors. The number of such channels is energy dependent and, except at $E = 0$, the number of particle channels $m_i^+(E)$ need not equal the number of hole channels $m_i^-(E)$. In what follows, the symbol l will be used to denote a triplet of quantum numbers (a, α, i), which define an α-type channel of lead i, with transverse k-vector of quantum number a. Thus $\alpha = +1(-1)$ for particles (holes), $i = 1, \ldots, n$ and $a = 1, 2, \ldots, m_i^\alpha(E)$. Having identified all possible channels, the S-matrix $S(E)$ of dimensionality $M(E) = \sum_{i=1}^{n} m_i(E) = \sum_{i=1}^{n}(m_i^+(E) + m_i^-(E))$ is defined by the relation

$$|\text{out}\rangle = S(E, \Delta, \boldsymbol{A}, U)|\text{in}\rangle \tag{4.3}$$

where $|\text{out}\rangle$ ($|\text{in}\rangle$) is a vector of outgoing (incoming) plane wave amplitudes, each amplitude being multiplied by the square root of its longitudinal group velocity to ensure unitarity of S. Clearly any scattering problem can be solved once S is known.

As an example of how S can be computed in practice, consider the one-dimensional system shown in figure 7. For this example, the S-matrix may be obtained after first introducing a transfer matrix T defined by

$$\begin{pmatrix} O' \\ I' \end{pmatrix} = T \begin{pmatrix} I \\ O \end{pmatrix} \tag{4.4}$$

where

$$\begin{pmatrix} O' \\ I' \end{pmatrix} = \hbar^{1/2} \begin{pmatrix} k^{1/2}A' \\ q^{1/2}D' \\ k^{1/2}B' \\ q^{1/2}C' \end{pmatrix} \tag{4.5a}$$

and

$$\begin{pmatrix} I \\ O \end{pmatrix} = \hbar^{1/2} \begin{pmatrix} k^{1/2}A \\ q^{1/2}D \\ k^{1/2}B \\ q^{1/2}C \end{pmatrix}. \tag{4.5b}$$

A range of iterative techniques are available [12, 13] for computing T, and once it is known the S-matrix satisfying

$$\begin{pmatrix} O \\ O' \end{pmatrix} = S \begin{pmatrix} I \\ I' \end{pmatrix} \tag{4.6}$$

can be constructed. Indeed if S is written as

$$S = \begin{pmatrix} r & t' \\ t & r' \end{pmatrix} \tag{4.7}$$

then T has the form

$$T = \begin{pmatrix} T_{11} & T_{12} \\ T_{21} & T_{22} \end{pmatrix} = \begin{pmatrix} (t^\dagger)^{-1} & r'(t')^{-1} \\ -(t')^{-1}r & (t')^{-1} \end{pmatrix} \tag{4.8}$$

from which the following inverse relation is obtained:

$$S = \begin{pmatrix} -T_{22}^{-1}T_{21} & T_{22}^{-1} \\ (T_{11}^\dagger)^{-1} & T_{12}T_{22}^{-1} \end{pmatrix}. \tag{4.9}$$

More generally, the above analysis remains valid for any two-probe system with d-dimensional leads of constant cross section, provided the four component column vectors introduced in (4.4) are replaced by $M(E)$ component vectors describing the $M(E)$ incoming and $M(E)$ outgoing channels the collection of leads.

Clearly $S(E, \Delta, A, U)$ is a functional of all physical potentials, as well as a function of E. Since H is Hermitian, quasi-particle probability is conserved, which yields

$$S^{-1}(E, \Delta, A, U) = S^{\dagger}(E, \Delta, A, U). \tag{4.10}$$

Furthermore, time reversal symmetry yields

$$S^{*}(E, \Delta^{*}, -A, U) = S^{-1}(E, \Delta, A, U) \tag{4.11}$$

and hence

$$S(E, \Delta^{*}, -A, U) = S^{t}(E, \Delta, A, U). \tag{4.12}$$

If a matrix P is constructed with elements $P_{ll'} = |S_{ll'}|^2$ and vectors $|\tilde{\text{out}}\rangle$, $|\tilde{\text{in}}\rangle$ of probability fluxes are formed with elements equal to the squared magnitudes of $|\text{out}\rangle$, $|\text{in}\rangle$, then the equation for outgoing fluxes due to incoming incoherent wavepackets is of the form

$$|\tilde{\text{out}}\rangle = P|\tilde{\text{in}}\rangle \tag{4.13}$$

where from (4.10)

$$\sum_{l'=1}^{M(E)} P_{ll'} = \sum_{l=1}^{M(E)} P_{ll'} = 1. \tag{4.14}$$

Furthermore, from (4.12), if Δ is real and $A = 0$, P is symmetric. To obtain expressions for transport coefficients, consider the $[m_j^{\beta}(E)m_i^{\alpha}(E)]$ matrix elements $P_{ll'}(E)$, where $l = (a, \alpha, i)$ and $l' = (b, \beta, j)$. Then the transition probability from all incoming β channels of lead j, energy E, to all outgoing α channels of lead i is

$$\bar{P}_{ij}^{\alpha\beta}(E) = \sum_{a,b} P_{ll'}(E). \tag{4.15}$$

Note that the elements $P_{ll'}(E)$ appearing in this equation form a sub-matrix $P_{ij}^{\alpha\beta}(E)$ of $P(E)$, with $m_i^{\alpha}(E)$ rows and $m_j^{\beta}(E)$ columns. The elements of $P_{ij}^{\alpha\beta}(E)$ are $[P_{ij}^{\alpha\beta}(E)]_{ab} = |[S_{ij}^{\alpha\beta}(E)]_{ab}|^2$, where $S_{ij}^{\alpha\beta}(E)$ is the corresponding sub-matrix of S and satisfies the particle–hole symmetry relation $P_{ij}^{\alpha\beta}(E) = P_{ij}^{-\alpha-\beta}(-E)$. Clearly, (4.15) can be written

$$\bar{P}_{ij}^{\alpha\beta}(E) = \mathrm{Tr}\{[S_{ij}^{\alpha\beta}(E)][S_{ij}^{\alpha\beta}(E)]^{\dagger}\}. \tag{4.16}$$

From (4.14) we see that

$$\sum_{i\alpha} \bar{P}_{ij}^{\alpha\beta}(E) = m_j^{\beta}(E) \tag{4.17a}$$

and

$$\sum_{j\beta} \bar{P}_{ij}^{\alpha\beta}(E) = m_i^{\alpha}(E). \tag{4.17b}$$

Taking into account the fact that, for each channel, the product of the density of states per unit length and the longitudinal group velocity is $2/h$, where h is the Planck constant, the number of incident quasi-particles per unit time of type β along lead j, with energies between E and $E + \Delta E$, is $J_j^\beta(E) = (2/h)m_j^\beta(E)f_j^\beta(E)$, where $f_j^\beta(E)$ is the distribution of incoming quasi-particles of type β, from reservoir j of temperature T_j and chemical potential μ_j. Similarly, from (4.15,) the number of outgoing α-type quasi-particles per unit time in lead i, with energies between E and $E + \Delta E$ is

$$\hat{J}_i^\alpha(E)\Delta E = (2/h)\sum_{j,\beta} \bar{P}_{ij}^{\alpha\beta}(E) f_j^\beta(E)\Delta E.$$

The total electrical current in lead i due to all quasi-particles between E and $E + \Delta E$ is therefore $e\hat{I}_i(E)\Delta E$, where

$$\hat{I}_i(E) = \sum_{\alpha=\pm 1} \alpha\big(J_i^\alpha(E) - \hat{J}_i^\alpha(E)\big) \tag{4.18}$$

while the total flux of energy in this interval is $E\hat{Q}_i(E)\Delta E$, where

$$\hat{Q}_i(E) = \sum_{\alpha=\pm 1} \big(J_i^\alpha(E) - \hat{J}_i^\alpha(E)\big). \tag{4.19}$$

Hence we obtain

$$\begin{pmatrix} \hat{\boldsymbol{I}}(E) \\ \hat{\boldsymbol{Q}}(E) \end{pmatrix} = \frac{2e}{h} \begin{pmatrix} m^+ - \bar{P}^{++}(E) + \bar{P}^{-+}(E) & -m^- + \bar{P}^{--}(E) - \bar{P}^{+-}(E) \\ m^+ - \bar{P}^{++}(E) - \bar{P}^{-+}(E) & m^- - \bar{P}^{--}(E) - \bar{P}^{+-}(E) \end{pmatrix} \begin{pmatrix} \boldsymbol{f}^+(E) \\ \boldsymbol{f}^-(E) \end{pmatrix} \tag{4.20}$$

where m^α is a diagonal matrix with elements $m_{ij}^\alpha = \delta_{ij} m_i^\alpha(E)$

This is a very general result, which as derived, applies to any mesoscopic system described by a time-independent Hamiltonian. Clearly, all transport properties of interest can be obtained from integrals of the form

$$\boldsymbol{I}^{(p)} = \int_0^\infty E^p \hat{\boldsymbol{I}}(E) \tag{4.21}$$

and

$$\boldsymbol{Q}^{(p)} = \int_0^\infty E^p \hat{\boldsymbol{Q}}(E) \tag{4.22}$$

where p is an integer. In particular, electrical transport properties are obtained from $e\boldsymbol{I}^{(0)}$, thermal transport properties from $\boldsymbol{Q}^{(1)}$ and combinations such as thermopower by standard methods [30]. For the case where $f_j^\alpha(E) = \{\exp[((E-\alpha(\mu_j-\mu))/k_\mathrm{B}T]+1\}^{-1}$, expanding in $\mu_j - \mu$ and retaining only the linear terms, yields (3.1), with

$$\begin{aligned} a_{ij} &= \frac{2e^2}{h}\int_0^\infty \frac{-\partial f(E)}{\partial E}[(m_j^+(E)\delta_{ij} - \bar{P}_{ij}^{++}(E) + \bar{P}_{ij}^{-+}(E) \\ &\qquad + (m_j^-(E) - \bar{P}_{ij}^{--}(E) + \bar{P}_{ij}^{+-}(E))] \\ &= \frac{2e^2}{h}\int_{-\infty}^\infty \frac{-\partial f(E)}{\partial E}[(m_j^+(E)\delta_{ij} - \bar{P}_{ij}^{++}(E) + \bar{P}_{ij}^{-+}(E)] \end{aligned} \tag{4.23}$$

where $f(E)$ is the Fermi function and the last step made use of particle–hole symmetry, $\bar{P}_{ij}^{\alpha\beta}(E) = \bar{P}_{ij}^{-\alpha-\beta}(-E)$. At zero temperature, where $-\partial f(E)/\partial E = \delta(E)$, this reduces to

$$a_{ij} = (2e^2/h)[m_j^+(0)\delta_{ij} - \bar{P}_{ij}^{++}(0) + \bar{P}_{ij}^{-+}(0)]. \tag{4.24}$$

For the case of two identical probes with $m_1^+(0) = m_2^+(0) = N$ channels, it is convenient to write

$$\bar{P}^{++}(0) = \begin{pmatrix} R_0 & T_0 \\ T_0' & R_0' \end{pmatrix} \tag{4.25}$$

$$\bar{P}^{-+}(0) = \begin{pmatrix} R_a & T_a \\ T_a' & R_a' \end{pmatrix}. \tag{4.26}$$

With this notation, the matrix of coefficients in (3.1) becomes (in units of $2e^2/h$)

$$A = \begin{pmatrix} a_{11} & a_{12} \\ a_{21} & a_{22} \end{pmatrix} = \begin{pmatrix} N - R_0 + R_a & T_a - T_0 \\ T_a' - T_0' & N - R_0' + R_a' \end{pmatrix}. \tag{4.27}$$

The coefficients R_0, T_0 (R_a, T_a) are probabilities for normal (Andreev) reflection and transmission for quasi-particles from reservoir 1, while R_0', T_0' (R_a', T_a') are corresponding probabilities for quasi-particles from reservoir 2. From (4.14), these are normalized to the number N of channels per quasi-particle type, per lead (in contrast with the normalization to unity in [15]) and satisfy

$$R_0 + T_0 + R_a + T_a = R_0' + T_0' + R_a' + T_a' = N \tag{4.28}$$

and

$$T_0 + T_a = T_0' + T_a'. \tag{4.29}$$

Clearly, unless all Andreev coefficients vanish, A possesses an inverse.

For this particular example, we find $x_1 = 2(T_a + R_a)$, $x_2 = 2(T_a' + R_a')$, $y_1 = 2(R_a + T_a')$ and $y_2 = 2(R_a' + T_a)$. Hence (3.9) yields [9]

$$G_{12}^{12} = N - R_0 + R_a - \frac{2(T_a + R_a)(T_a' + R_a)}{T_a + R_a + T_a' + R_a'} = T_0 + T_a + \frac{2(R_a R_a' - T_a T_a')}{R_a + R_a' + T_a + T_a'}. \tag{4.30}$$

Similarly (3.11) for the condensate potential reduces to

$$V = V_1 + (V_1 - V_2)(R_a + T_a')/(R_a + R_0 + T_a + T_a'). \tag{4.31}$$

It is interesting to note that, for this example, the probability flux $\hat{Q}(0)$ of (4.20) is given by

$$\hat{Q}_1(0) = \hat{Q}_2(0) = (\mu_1 - \mu_2)(T_0 + T_a)(2/h) \tag{4.32}$$

and therefore if one introduces a 'probability conductance' defined by $G_d = \hat{Q}_1/[2(\mu_1 - \mu_2)/h]$, one obtains

$$G_d = T_0 + T_a = \mathrm{Tr}\,\{tt^\dagger\} \tag{4.33}$$

where t is the lower left-hand sub-matrix of the multi-channel S-matrix of (4.7). Thus it is G_d rather than the electrical conductance which satisfies the well-known two-probe Büttiker formula in the presence of Andreev scattering. Since G_d is closely related to quasi-particle diffusion and thermal conductance, this result leads one to expect that the latter will exhibit many of the properties associated with the electrical conductance of normal mesoscopic systems, such as universal conductance fluctuations and localization phenomena.

The electrical conductance, on the other hand, is distinct from quasi-particle diffusion and therefore many of the standard results from the theory of transport in normal systems may be modified. This separation of diffusion and electrical conductance is highlighted by combining (4.30) and (4.32) to yield

$$G_{12}^{12} = G_d + 2(R_a R_a' - T_a T_a')/(R_a + R_a' + T_a + T_a'). \tag{4.34}$$

In the limit of zero diffusion (i.e. transmission), where G_d vanishes, this reduces to

$$G_{12}^{12} = 1/[(2R_a)^{-1} + (2R_a')^{-1}]. \tag{4.35}$$

Hence, as noted in section 3, in this limit the two-probe resistance reduces to a sum of two boundary resistances, reflecting the fact that even in the absence of diffusion, electrical current can flow from one reservoir to the other, through the exchange of charge between quasi-particles and the condensate at the normal–superconducting interfaces. The expression $(2R_a)^{-1}$ for the boundary resistance of a single interface was first derived by Blonder and co-workers [24].

5. Discussion

Having obtained generalized formulae for transport coefficients in terms of S-matrix elements, we end by briefly remarking on how the latter can be obtained, once the potentials $U(\boldsymbol{r})$, $\Delta(\boldsymbol{r})$ and $\boldsymbol{A}(\boldsymbol{r})$ of (4.2) are known. To compute the S-matrix analytically, we write the Bogoliubov–de Gennes operator of (4.2) in the form $\boldsymbol{H}(\boldsymbol{r}) = \boldsymbol{H}_0(\boldsymbol{r}) + \boldsymbol{H}_1(\boldsymbol{r})$, where $\boldsymbol{H}_0(\boldsymbol{r})$ is diagonal and make use of the following 'golden rule', which was first written down in [9] and is generalized to many probes in appendix A:

$$S_{ll'}(E) = S_{ll'}^0(E) + T_{ll'}^+(E) = i\hbar[v_l(E)v_{l'}(E)]^{1/2}\bar{G}_{ll'}^+(E). \tag{5.1}$$

In this expression, $S_{ll'}^0(E)$ is the S-matrix of the normal system described by $\boldsymbol{H}_0$, $T_{ll'}^+(E)$ is the T-matrix describing the additional scattering by $\boldsymbol{H}_1$ and $\bar{G}_{ll'}^+(E)$ is the full Green function of the hybrid structure. To compute the S-matrix numerically, perhaps the most efficient method is based on the transfer matrix technique, described in appendix B.

Equations (3.5) and (3.7), when combined with (4.13) and the S-matrix formulae of appendices A and B, form a complete description of DC transport, in systems with dimensions less than the inelastic scattering length. Of course, the potentials to be used in (4.2) should strictly be the fully self-consistent steady state values. In practice, these will only be known for the simplest cases and one will usually be forced to use non-self-consistent forms, which capture the essential physics. Many examples of such choices are to be found in the literature [6–14]. The analysis presented here will, for the first time, allow ideas developed in these and other articles to be extended to multi-probe transport measurements.

The central results of this paper, namely equations (3.5)–(3.7), are a generalization of the original work of [15] and build upon intuitive ideas developed for normal mesoscopic systems [17, 18]. For normal systems, such formulae can be derived from an alternative viewpoint [31], which starts from the Kubo formula. For the future it would be of interest to obtain a corresponding derivation, valid for mesoscopic superconductors.

Acknowledgments

This work is supported by the SERC, the EC HCM programme, a NATO collaborative research grant and the MOD. It has benefited from conversations with J H Jefferson, J-L Pichard and B Kramer.

Appendix A. Golden rules for S-matrix coefficients

To obtain analytic results for S-matrix coefficients, we write the Bogoliubov–de Gennes operator of (4.2) in the form $\boldsymbol{H}(\boldsymbol{r}) = \boldsymbol{H}_0(\boldsymbol{r}) + \boldsymbol{H}_1(\boldsymbol{r})$, where $\boldsymbol{H}_0(\boldsymbol{r})$ is diagonal. In what follows 2×2 operators, such as $\boldsymbol{H}(\boldsymbol{r})$, will be denoted by bold italic characters and two-component vectors, such as the right-hand side of (4.2), will be denoted by bold Greek symbols.

Consider first a translationally invariant system, formed by joining two semi-infinite leads j, j' of equal cross section and described by the kinetic energy operator $\boldsymbol{h}_0(\boldsymbol{r})$ obtained by setting $U(\boldsymbol{r}) = \Delta(\boldsymbol{r}) = 0$ on the right-hand side of (4.2). The eigenstates of $\boldsymbol{h}_0(\boldsymbol{r})$ corresponding to a unit quasi-particle flux of type β, energy E, incident along channel b of lead j, are plane waves of the form

$$\boldsymbol{\phi}_{j,E}^{\beta,b}(\boldsymbol{r}) = \delta_{\beta,+1} \begin{pmatrix} 1 \\ 0 \end{pmatrix} \phi_{j,E}^{+,b}(\boldsymbol{r}) + \delta_{\beta,-1} \begin{pmatrix} 0 \\ 1 \end{pmatrix} \phi_{j,E}^{-,b}(\boldsymbol{r}) \qquad \text{(A.1)}$$

Under an adiabatic change to the normal multi-probe system described by $\boldsymbol{H}_0(\boldsymbol{r})$, such a state evolves into an eigenstate $\boldsymbol{\psi}_{j,E}^{\beta,b}(\boldsymbol{r})$ of $\boldsymbol{H}_0(\boldsymbol{r})$, of the form

$$\boldsymbol{\psi}_{j,E}^{\beta,b}(\boldsymbol{r}) = \delta_{\beta,+1} \begin{pmatrix} 1 \\ 0 \end{pmatrix} \psi_{j,E}^{+,b}(\boldsymbol{r}) + \delta_{\beta,-1} \begin{pmatrix} 0 \\ 1 \end{pmatrix} \psi_{j,E}^{-,b}(\boldsymbol{r}). \qquad \text{(A.2)}$$

Note that, except for the case of two identical leads, even if $\boldsymbol{H}_0(\boldsymbol{r})$ is chosen to be the kinetic energy operator, $\boldsymbol{\psi}_{j,E}^{\beta,b}(\boldsymbol{r}) \neq \boldsymbol{\phi}_{j,E}^{\beta,b}(\boldsymbol{r})$, because the former includes the effect of scattering from boundaries between leads.

Using the solutions (A.2) as a starting point, the corresponding exact wavefunction $\boldsymbol{\Psi}_{j,E}^{\beta,b}(\boldsymbol{r})$ arising when $\boldsymbol{H}_1(\boldsymbol{r}) \neq 0$ is given by

$$\boldsymbol{\Psi}_{j,E}^{\beta,b}(\boldsymbol{r}) = \boldsymbol{\psi}_{j,E}^{\beta,b}(\boldsymbol{r}) + \bar{\boldsymbol{\Psi}}_{j,E}^{\beta,b}(\boldsymbol{r}) \qquad \text{(A.3)}$$

where the additional contribution to the outgoing scattered wavefunction of the superconducting system is

$$\bar{\boldsymbol{\Psi}}_{j,E}^{\beta,b}(\boldsymbol{r}) = \int \mathrm{d}^3 r' \boldsymbol{G}^{+}(\boldsymbol{r}, \boldsymbol{r}', E) \boldsymbol{H}_1(\boldsymbol{r}') \boldsymbol{\Psi}_{j,E}^{\beta,b}(\boldsymbol{r}'). \qquad \text{(A.4)}$$

In this equation, for a given choice of $\boldsymbol{H}_0(\boldsymbol{r})$, the 2×2 matrix $\boldsymbol{H}_1(\boldsymbol{r})$ is defined by $\boldsymbol{H}_1(\boldsymbol{r}) = \boldsymbol{H}(\boldsymbol{r}) - \boldsymbol{H}_0(\boldsymbol{r})$ and $\boldsymbol{G}^{\pm}(\boldsymbol{r}, \boldsymbol{r}', E)$ denotes a Green function belonging to $\boldsymbol{H}_0(\boldsymbol{r})$:

$$\boldsymbol{G}^{\pm}(\boldsymbol{r}, \boldsymbol{r}', E) = \begin{pmatrix} G_{+}^{\pm}(\boldsymbol{r}, \boldsymbol{r}', E) & 0 \\ 0 & G_{-}^{\pm}(\boldsymbol{r}, \boldsymbol{r}', E) \end{pmatrix} \qquad \text{(A.5)}$$

where subscripts + (−) refer to particles (holes) and superscripts + (−) refer to causal (anti-causal) Green functions.

If $l' = (b, \beta, j)$ labels an incoming β-type quasi-particle channel, with transverse quantum number b of lead j and $l = (a, \alpha, i)$ labels an outgoing channel of lead i, then since the S-matrix coefficient $S_{ll'}(E) = [S_{ij}^{\alpha,\beta}(E)]_{a,b}$ is obtained by projecting the outgoing asymptotic part of $\boldsymbol{\Psi}_{j,E}^{\beta,b}(\boldsymbol{r})$ onto channel l, we find

$$S_{ll'}(E) = v_l(E) \int \mathrm{d}^2 \rho_i \, [\boldsymbol{\phi}_{i,E}^{\alpha,a}(\beta_i + \rho_i)]^{\dagger} [\boldsymbol{\Psi}_{j,E}^{\beta,b}(\beta_i + \rho_i) - \delta_{i,j} \boldsymbol{\phi}_{j,E}^{\beta,b}(\beta_i + \rho_i)]. \qquad \text{(A.6)}$$

In this expression, $v_l(E)$ is the group velocity for channel l and a position vector in lead i has been written $\boldsymbol{r}_i = (\boldsymbol{\beta}_i + \boldsymbol{\rho}_i)$, where $\boldsymbol{\beta}_i$ ($\boldsymbol{\rho}_i$) is parallel (perpendicular) to the walls of lead i. In (A.6), the presence of the term $\phi^{\beta,b}_{j,E}(\boldsymbol{\beta}_i + \boldsymbol{\rho}_i)$ removes any contribution from the incoming wave along channel l'. The pre-factor $v_l(E)$ arises from a term $v_l(E)^{1/2}$, which converts an outgoing intensity into an outgoing flux, and a second factor $v_l(E)^{1/2}$, which corrects for the fact that the projection is carried out using a state $\phi^{\alpha,a}_{i,E}$ normalized to unit flux rather than unit amplitude. Indeed, for leads of constant cross section, an incoming plane wave of unit flux can be written

$$\phi^{\beta,b}_{j,E}(\boldsymbol{\beta}_j + \boldsymbol{\rho}_j) = \chi^b_j(\boldsymbol{\rho}_j)\,[v_{l'}(E)]^{-1/2}\exp(\mathrm{i}k^{\beta,b}_j(E)\eta_j) \tag{A.7}$$

where $\chi^b_j(\boldsymbol{\rho}_j)$ is the transverse mode of channel l' and $(v_{l'}(E))^{-1/2}\exp(ik^{\beta,b}_j(E)\eta_j)$ is a plane wave of unit flux, with longitudinal wavevector $k^{\beta,b}_j(E)$, whose sign is chosen such that $\phi^{\beta,b}_{j,E}(\boldsymbol{\beta}_j + \boldsymbol{\rho}_j)$ an incoming wave. For example, in the case of two rectangular leads of cross sectional area $d^j_1 \times d^j_2$, aligned parallel to the x axis, $\boldsymbol{\rho}$ is replaced by cartesian components y, z to yield

$$\chi^b_j(y,z) = 2(d^j_1\, d^j_2)^{-1/2}\sin n_b\pi y/d^j_1\ \sin n'_b\pi z/d^j_2 \tag{A.8}$$

and η_j becomes the cartesian component x.

Combining (A.6) and (A.7) yields the following exact result for S-matrix coefficients:

$$\begin{aligned} S_{ll'}(E) = [S^{\alpha\beta}_{ij}]_{a,b} = v_l(E)^{1/2}\exp[\mathrm{i}k^{\alpha,a}_i(E)\eta_i]\int \mathrm{d}^2\rho_i\ \chi^a_i(\boldsymbol{\rho}_i)(\delta_{\alpha,1}\ \delta_{\alpha,-1}) \\ \times [\Psi^{\beta,b}_{j,E}(\boldsymbol{\beta}_i + \boldsymbol{\rho}_i) - \delta_{i,j}\phi^{\beta,b}_{j,E}(\boldsymbol{\beta}_i + \boldsymbol{\rho}_i)]. \end{aligned} \tag{A.9}$$

Since open channels are orthogonal to evanescent closed channels, η_i can be chosen to be any position within lead i, outside the scattering region. Furthermore, since the quantity in square brackets is outgoing, while $\exp[\mathrm{i}k^{\alpha,a}_i(E)\eta_i]$ is incoming, the phase factors cancel to yield a result which is independent of η_i. After evaluating the right-hand side of (A.9), the coefficients $\bar{P}^{\alpha\beta}_{ij}(E)$ of (4.16) can be computed. All reflection (transmission) coefficients are obtained by choosing $i = j$ ($i \neq j$) and all normal (Andreev) coefficients from the choice $\alpha = \beta$ ($\alpha \neq \beta$).

Equation (A.9) forms a convenient starting point for developing series expansions in powers of Δ. To lowest order in Δ, it is clear from (A.4) and (A.6) that all Andreev scattering coefficients, which correspond to $\alpha \neq \beta$, are of order $|\Delta|^2$. To obtain higher-order results, we note that from (A.3) and (A.4)

$$\Psi^{\beta,b}_{j,E}(\boldsymbol{r}) = \psi^{\beta,b}_{j,E}(\boldsymbol{r}) + \int \mathrm{d}^3r'\mathrm{d}^3r''\ \boldsymbol{G}^+(\boldsymbol{r},\boldsymbol{r}',E)\boldsymbol{T}^+(\boldsymbol{r}',\boldsymbol{r}'',E)\psi^{\beta,b}_{j,E}(\boldsymbol{r}'') \tag{A.10}$$

where

$$\boldsymbol{T}^\pm(\boldsymbol{r},\boldsymbol{r}',E) = \boldsymbol{H}_1(\boldsymbol{r})\delta(\boldsymbol{r}-\boldsymbol{r}') + \int \mathrm{d}^3r''\boldsymbol{H}_1(\boldsymbol{r})\boldsymbol{G}^\pm(\boldsymbol{r},\boldsymbol{r}'',E)\boldsymbol{T}^\pm(\boldsymbol{r}'',\boldsymbol{r}',E). \tag{A.11}$$

Hence

$$S_{ll'}(E) = S^0_{ll'}(E) + T^+_{ll'}(E) \tag{A.12}$$

where $S^0_{ll'}(E)$ is obtained by substituting ψ for Ψ on the right-hand side of (A.9) and

$$T^+_{ll'}(E) = [v_l(E)]^{1/2}\exp[\mathrm{i}k_i^{\alpha,a}(E)\eta_i] \times \int \mathrm{d}^2\rho_i \mathrm{d}^3r' \mathrm{d}^3r'' \chi_i^a(\rho_i) G^+_\alpha(\boldsymbol{r}_i, \boldsymbol{r}', E) T^+_{\alpha\beta}(\boldsymbol{r}', \boldsymbol{r}'', E)\psi^{\beta,b}_{j,E}(\boldsymbol{r}''). \tag{A.13}$$

The 'golden rule' (A.13) and can be simplified by exploiting the intimate relationship between Green functions and scattering states. To illustrate this, consider again the system shown in figure 6(a) and described by $h_0(\boldsymbol{r})$, which possesses plane wave eigenstates $\phi^{\beta,b}_{j,E}(\boldsymbol{r})$ and a diagonal causal Green function $g^+(\boldsymbol{r}, \boldsymbol{r}', E)$, with elements

$$g_{\alpha\beta}(\boldsymbol{r}, \boldsymbol{r}', E) = \delta_{\alpha,\beta} g^+_\beta(\boldsymbol{r}, \boldsymbol{r}', E) = \delta_{\alpha,\beta} \sum_{b=1}^{\infty} \chi_j^b(\rho)\chi_j^b(\rho')[\mathrm{i}\hbar v_{l'}(E)]^{-1}\exp[\mathrm{i}k_j^{\beta,b}(E)\,|\eta - \eta'|]. \tag{A.14}$$

Under an adiabatic change from figure 6(a) to the scattering system described by $\boldsymbol{H}_0(\boldsymbol{r})$, the state $\phi^{\beta,b}_{j,E}(\boldsymbol{r})$ evolves to the scattering state $\psi^{\beta,b}_{j,E}(\boldsymbol{r})$ of (A.3). Hence the two-component vector

$$\begin{pmatrix} \delta_{\beta,+} \\ \delta_{\beta,-} \end{pmatrix} f_\beta(\boldsymbol{r}, \boldsymbol{r}', E)$$

where

$$f_\beta(\boldsymbol{r}, \boldsymbol{r}', E) = \sum_{b=1}^{\infty} \chi_j^b(\rho')[\mathrm{i}\hbar(v_{l'}(E))^{1/2}]^{-1}\exp[-\mathrm{i}k_j^{\beta,b}(E)\eta']\phi^{\beta,b}_{j,E}(\boldsymbol{r}) \tag{A.15}$$

evolves to the vector

$$\begin{pmatrix} \delta_{\beta,+} \\ \delta_{\beta,-} \end{pmatrix} G^+_\beta(\boldsymbol{r}, \boldsymbol{r}', E) = \sum_{b=1}^{\infty} \chi_j^b(\rho')[\mathrm{i}\hbar(v_{l'}(E))^{1/2}]^{-1}\exp[-\mathrm{i}k_j^{\beta,b}(E)\eta']\psi^{\beta,b}_{j,E}(\boldsymbol{r}). \tag{A.16}$$

Provided $\boldsymbol{r}$ and $\boldsymbol{r}'$ are chosen such that, in the scattering region, the right-hand sides of (A.14) and (A.15) are equal, (A.16) relates the Green function $G^+_{\alpha\beta} = \delta_{\alpha,\beta}G^+_\beta$ to an eigenstate ψ of the normal system. In what follows, for $\boldsymbol{r}'$ located in lead j, this restriction on $\boldsymbol{r}, \boldsymbol{r}'$ will be denoted $\{\boldsymbol{r}' = \boldsymbol{r}_j,\ \boldsymbol{r} > \boldsymbol{r}'\}$. If $\boldsymbol{r}'$ is located in lead j, then the condition $\boldsymbol{r} > \boldsymbol{r}'$ implies that $\boldsymbol{r}$ is arbitrary, apart from the restriction that if $\boldsymbol{r}$ is also in lead j, $\boldsymbol{r}$ must be closer to the scatterer than $\boldsymbol{r}'$. With this definition, from (A.16), for $\{\boldsymbol{r}' = \boldsymbol{r}_i,\ \boldsymbol{r} > \boldsymbol{r}'\}$, the following quantity yields the wavefunctions of the normal system:

$$\mathrm{G}^+_{\alpha,a,i}(\boldsymbol{r}, E) = \exp[\mathrm{i}k_i^{\alpha a}(E)\eta'] \int \mathrm{d}^2\rho'\ G^+_\alpha(\boldsymbol{r}, \boldsymbol{r}', E)\chi_i^a(\rho') = [\mathrm{i}\hbar(v_l(E))^{1/2}]^{-1}\psi^{\alpha,a}_{i,E}(\boldsymbol{r}). \tag{A.17}$$

As it stands, (A.17) could be used to eliminate $\psi^{\beta,b}_{j,E}(\boldsymbol{r}'')$ from the right-hand side of (A13), but not to replace G^+_α in the latter by a wavefunction. This is because in the integrand of (A13), $\{\boldsymbol{r}' > \boldsymbol{r}_i\}$, while in (A.17), $\{\boldsymbol{r}' = \boldsymbol{r}_i,\ \boldsymbol{r} > \boldsymbol{r}'\}$. To eliminate G^+_α from (A.13), we note that since $\boldsymbol{H}_0$ is Hermitian

$$[G^+_\alpha(\boldsymbol{r}, \boldsymbol{r}', E)]^* = G^-_\alpha(\boldsymbol{r}', \boldsymbol{r}, E). \tag{A.18}$$

Furthermore, provided $\boldsymbol{H}_0$ is chosen to be real, particle–hole symmetry yields

$$G_\alpha^+(\boldsymbol{r}, \boldsymbol{r}', E) = -G_{-\alpha}^-(\boldsymbol{r}, \boldsymbol{r}', -E) \tag{A.19}$$

which combines with (A.18) to yield

$$G_\alpha^+(\boldsymbol{r}, \boldsymbol{r}', E) = [-G_{-\alpha}^+(\boldsymbol{r}', \boldsymbol{r}, -E)]^*. \tag{A.20}$$

Noting that $k_i^{-\alpha a}(-E) = -k_i^{\alpha a}(E)$ and since all v_l are defined to be positive, $v_{-\alpha,a,i}(-E) = v_{\alpha,a,i}(E)$, (A.20) and (A.15) combine to yield $\{\boldsymbol{r}' = \boldsymbol{r}_i,\ \boldsymbol{r} > \boldsymbol{r}'\}$

$$[\mathrm{i}\hbar(v_l(E))^{1/2}]^{-1}[\psi_{i,-E}^{-\alpha,a}(\boldsymbol{r})]^* = \exp[\mathrm{i}k_i^{\alpha a}(E)\eta'] \int \mathrm{d}^2\rho'\ G_\alpha^+(\boldsymbol{r}, \boldsymbol{r}', E)\chi_i^a(\rho'). \tag{A.21}$$

This allows (A.13) to be written, for real $\boldsymbol{H}_0$, as

$$T_{ll'}^+(E) = (\mathrm{i}\hbar)^{-1} \int \mathrm{d}^3r'\mathrm{d}^3r''[\psi_{i,-E}^{-\alpha,a}(\boldsymbol{r}')]^* T_{\alpha\beta}^+(\boldsymbol{r}', \boldsymbol{r}'', E)\psi_{j,E}^{\beta,b}(\boldsymbol{r}'') \tag{A.22a}$$

or equivalently, for real $\boldsymbol{H}_0$, as

$$T_{ll'}^+(E) = -\mathrm{i}\hbar[v_l(E)v_{l'}(E)]^{1/2} \int \mathrm{d}^3r'\mathrm{d}^3r''[G_{-\alpha,a,i}^+(\boldsymbol{r}', -E)]^* T_{\alpha\beta}^+(\boldsymbol{r}', \boldsymbol{r}'', E) G_{\beta,b,j}^+(\boldsymbol{r}'', E). \tag{A.22b}$$

Equations (A.9) and (A.12) are equivalent expressions for the scattering matrix of a mesoscopic superconductor. Equation (A.12) expresses the full S-matrix as a sum of the scattering matrix S^0 of $\boldsymbol{H}_0$ and a contribution to scattering from the superconducting order parameter embodied in the solution to (A.11). If $\boldsymbol{H}_0(\boldsymbol{r})$ is chosen to equal $h_0(\boldsymbol{r})$, then S^0 is diagonal and all non-trivial scattering is contained in $T_{ll'}^+(E)$. If $\boldsymbol{H}_0(\boldsymbol{r})$ is chosen to be the 2×2 matrix obtained by setting $\Delta(\boldsymbol{r}) = 0$ on the right-hand side of (4.2), then $\boldsymbol{H}_0(\boldsymbol{r})$ and therefore S^0 describes the scattering of incident plane waves of the normal 'background' material. This latter choice renders $\boldsymbol{H}_1(\boldsymbol{r})$ off-diagonal and to order Δ^2 yields

$$\boldsymbol{T}^+(\boldsymbol{r}, \boldsymbol{r}') = \begin{pmatrix} \Delta(\boldsymbol{r})G_-^+(\boldsymbol{r}, \boldsymbol{r}', E)\Delta^*(\boldsymbol{r}') & \delta(\boldsymbol{r} - \boldsymbol{r}')\Delta(\boldsymbol{r}) \\ \delta(\boldsymbol{r} - \boldsymbol{r}')\Delta^*(\boldsymbol{r}) & \Delta(\boldsymbol{r})G_+^+(\boldsymbol{r}, \boldsymbol{r}', E)\Delta(\boldsymbol{r}') \end{pmatrix}. \tag{A.23}$$

When combined with (A22a) and (A12), this is particularly useful when investigating changes in transport properties due to the onset of superconductivity. For completeness one also notes that a third expression for $S_{ll'}(E)$ is obtained from the result corresponding to (A.16) for the full Green function $\tilde{G}^+(\boldsymbol{r}, \boldsymbol{r}', E)$ of the superconducting system, satisfying

$$(E\boldsymbol{I} - \boldsymbol{H}(\boldsymbol{r}))\tilde{G}^\pm(\boldsymbol{r}, \boldsymbol{r}', E) = \delta(\boldsymbol{r} - \boldsymbol{r}')\boldsymbol{I}$$

where $\boldsymbol{I}$ is a 2×2 unit matrix. The same argument which led to (A16) shows that provided $\{\boldsymbol{r}' = \boldsymbol{r}_j,\ \boldsymbol{r} > \boldsymbol{r}'\}$

$$\begin{pmatrix} \tilde{G}_{+\beta}^+(\boldsymbol{r}, \boldsymbol{r}', E) \\ \tilde{G}_{-\beta}^+(\boldsymbol{r}, \boldsymbol{r}', E) \end{pmatrix} = \sum_{b=1}^{\infty} \chi_j^b(\rho')[\mathrm{i}\hbar(v_{l'}(E))^{1/2}]^{-1}\exp[-\mathrm{i}k_j^{\beta,b}(E)\eta']\Psi_{j,E}^{\beta,b}(\boldsymbol{r}). \tag{A.24}$$

In view of (A.9), for $\{\boldsymbol{r}' = \boldsymbol{r}_j,\ \boldsymbol{r} = \boldsymbol{r}_i,\ \boldsymbol{r} > \boldsymbol{r}'\}$, we define

$$\tilde{G}^{+}_{ll'}(E) = \exp \mathrm{i}[k_j^{\beta b}(E)\eta' + k_i^{\alpha a}(E)\eta] \int \mathrm{d}^2\rho \mathrm{d}^2\rho'\ \chi_i^a(\rho_i)\tilde{G}^{+}_{\alpha\beta}(\boldsymbol{r}, \boldsymbol{r}', E)\chi_j^b(\rho') \\ - \{\mathrm{i}\hbar[v_l(E)v_{l'}(E)]^{1/2}\}^{-1}\delta_{l,l'}\exp \mathrm{i}[2k_i^{\alpha a}(E)\eta]. \tag{A.25}$$

Then (A.9) reduces to (for real or complex $\boldsymbol{H}_0$)

$$S_{ll'}(E) = \mathrm{i}\hbar[v_l(E)v_{l'}(E)]^{1/2}\tilde{G}^{+}_{ll'}(E). \tag{A.26}$$

This could have been derived by substituting (A17) into (A13), and expresses scattering matrix elements in terms of off-diagonal elements of the full Green function of the hybrid system.

Appendix B. Numerical evaluation of the S-matrix

To obtain the S-matrix numerically, a simple approach is to compute the multi-channel T-matrix of (4.4) and then evaluate S via (4.9). To construct T in one dimension, it is convenient to consider stepwise functions $U(x)$ and $\Delta(x)$, which change only at a sequence of N_s steps. In this case, by insisting that a solution to (4.1) is continuous and has a continuous first derivative, the 4×4 transfer matrix T_j for step j can be obtained by matching solutions on either side of the discontinuity. The transfer matrix for the whole scatterer is then of the form

$$T = \prod_{j=1}^{N_s} T_j. \tag{B.1}$$

To construct T in more than one dimension, a simple technique is to map (4.1) onto an equivalent tight-binding problem by discretizing the Laplacian. For example, in three dimensions a simple cubic lattice with lattice constant a is introduced and $-\nabla^2\psi(x, y, z)$ is replaced by

$$a^{-2}\sum_{l=\pm 1}\{[\psi(x, y, z) - \psi(x + la, y, z)] + [\psi(x, y, z) - \psi(x, y + la, z)] \\ + [\psi(x, y, z) - \psi(x + la, y, z + la)]\}.$$

Clearly, the energy $\gamma = \hbar^2 a^{-2}/2m$, which plays the role of a tight-binding hopping matrix element, should be much larger than a typical value of $\Delta(\boldsymbol{r})$.

With the above replacement, for a lattice of N_c points, the Hamiltonian H becomes a $2N_c \times 2N_c$ matrix of the form

$$H = \begin{pmatrix} H_0 & H_1 \\ H_1^{\dagger} & -H_0^{*} \end{pmatrix} \tag{B.2}$$

where H_0 $(-H_0^*)$ is a $N_c \times N_c$ tight-binding matrix describing the particle (hole) degrees of freedom of the normal system and H_1 is a diagonal on-site particle–hole coupling matrix with elements $(H_1)_{jj} = \Delta(\boldsymbol{r}_j)$. More generally, if instead of a continuum Hamiltonian such as the top left-hand element of (4.2), one wishes to model the normal system by an arbitrary tight-binding Hamiltonian H_0, then (5.2) should be regarded as a starting point for such a model, rather a discrete approximation to a continuum limit.

As an example, for a scatterer of length N_1 sites and width N_2 sites, the T matrix of order $M(E)$ appearing in (4.8) and (4.9) is obtained by first evaluating a product $\bar{T}$ of N_1 complex transfer matrices, each of order $4N_2$, corresponding to the N_1 slices forming the scatterer and then identifying T with the sub-matrix of $\bar{T}$ corresponding to open channels only. To maintain numerical stability, the product must be Gram–Schmidt orthogonalized after each step. Otherwise the result is dominated by the largest eigenvalue and the matrix inversions in (4.9) will fail.

References

[1] Kramer B 1990 *Adv. Solid State Phys.* **30** 53
[2] Al'tshuler B L, Lee P A and Webb R A (ed) 1991 *Mesoscopic Phenomena in Solids* (Amsterdam: North-Holland)
[3] van Wees B J *et al* 1988 *Phys. Rev. Lett.* **60** 848
[4] Wharam D A *et al* 1988 *J. Phys. C: Solid State Phys.* **21** L209
[5] Garfunkel G A, Alers G B and Weissman M B 1990 *Phys. Rev.* B **41** 4901
[6] Beenakker C W J and van Houten H 1991 *Phys. Rev. Lett.* **66** 3056
[7] Glazman L I and Matveev K A 1989 *Sov. Phys.–JETP Lett.* **49** 659
[8] Beenakker C W J 1991 *Phys. Rev. Lett.* **67** 3836
[9] Lambert C J 1993 *J. Phys.: Condens. Matter* **5**
[10] Al'tshuler B L and Spivak B Z 1987 *Sov. Phys.–JETP* **65** 343
[11] Spivak B Z and Khmel'nitskii D E 1982 *Sov. Phys.–JETP Lett.* **35** 413
[12] Hui V C and Lambert C J 1990 *J. Phys.: Condens. Matter* **2** 7303
[13] Hui V C and Lambert C J 1993 *J. Phys.: Condens. Matter* **4**
[14] Ziegler K 1992 *Z. Phys.* B **86** 33
[15] Lambert C J 1990 *J. Phys.: Condens. Matter* **3** 6579
[16] Landauer R 1970 *Phil. Mag.* **21** 863
[17] Büttiker M, Imry Y, Landauer R and Pinhas S 1985 *Phys. Rev.* B **31** 6207
[18] Büttiker M 1988 *IBM J. Res. Develop.* **32** 317
[19] Clarke J, Eckern U, Schmid A, Shön G and Tinkham M 1979 *Phys. Rev.* B **20** 3933
[20] Tinkham M and Clarke J 1972 *Phys. Rev. Lett.* **28** 1368
[21] Tinkham M 1972 *Phys. Rev.* B **6** 1747
[22] Andreev A F 1964 *Sov. Phys.–JETP* **19** 1228
[23] Takane Y and Ebisawa H 1991 *J. Phys. Soc. Japan* **60** 3130
[24] Blonder G E, Tinkham M and Klapwijk T M 1982 *Phys. Rev.* B **25** 4515
[25] Beenakker C W E 1993 Preprint
[26] Fierz C, Lee S F, Bass J, Pratt W P Jr and Schroeder P A 1990 *J. Phys.: Condens. Matter* **2** 9701
[27] Lee S F, Pratt Jr W P, Lolee R, Schroeder P A and Bass J 1993 Preprint
[28] Schwarzbek S M and Ruggiero S T 1993 Preprint
[29] Lean H W and Waldram J R 1989 *J. Phys.: Condens. Matter* **1** 1299
[30] Ashcroft N W and Mermin N D 1976 *Solid State Physics* (New York: Holt, Rienhart and Winston)
[31] Stone A D and Szafer A 1988 *IBM J. Res. Develop.* **32** 384